Article

Not peer-reviewed version

Isolation, Identification, and Condition Optimization of an Ammonia-Oxidizing Bacterium and Its Potential Application in Wastewater Treatment

Yi-Lin Song , Hong-Fei Wang , Wei-Jin Zhang , Zhu Li , Jian Gao , Feng Guo , Lei Wu , Ming-Jun Liao *

Posted Date: 11 May 2026

doi: 10.20944/preprints202605.0679.v1

Keywords: ammonia-oxidizing bacteria; *Nitrosomonas europaea*; medium optimization; landfill leachate

 doi:10.20944/preprints202605.0679.v1

Article

Isolation, Identification, and Condition Optimization of an Ammonia-Oxidizing Bacterium and Its Potential Application in Wastewater Treatment

Yi-Lin Song [1], Hong-Fei Wang [1], Wei-Jin Zhang [1], Zhu Li [1], Jian Gao [1], Feng Guo [2], Lei Wu [2] and Ming-Jun Liao [1,*]

[1] Key Laboratory of Intelligent Perception and Ecological Restoration of River and Lake Health, Ministry of Education; Hubei Key Laboratory of Environmental Geotechnology and River-Lake Ecological Restoration; College of Civil Engineering, Architecture and Environment, Hubei University of Technology, Wuhan 430068, Hubei, China

[2] Gezhouba Group Ecological Environmental Protection Co., Ltd., Wuhan 430030, Hubei, China

* Correspondence: lmj1112@163.com

Abstract

Ammonia-oxidizing bacteria (AOB) are vital for the nitrogen cycle and wastewater treatment, yet their recalcitrance to isolation and cultivation hampers industrial application. To isolate an efficient strain and optimize its culture conditions for high-ammonia wastewater treatment, we collected water samples from a polluted river in Zhongshan City. After enrichment, a strain was isolated via gradient dilution and silica gel plating, identified by scanning electron microscopy and 16S rDNA sequencing as *Nitrosomonas europaea* W4 (99.93% similarity to the type strain). Single-factor medium optimization examined $CaCO_3$ and Fe^{2+}/Fe^{3+}, while temperature and initial ammonia nitrogen effects were tested, and landfill leachate was used for verification. $CaCO_3$ shortened the lag phase without affecting maximum specific growth rate; replacing Fe^{3+} with Fe^{2+} further reduced lag and enhanced the ammonia oxidation rate. Optimal growth occurred at 25–30 °C and an initial ammonia nitrogen concentration of ~2000 mg/L. In landfill leachate, the strain increased the ammonia degradation rate 6.3-fold. Overall, *N. europaea* W4 exhibits high ammonia oxidation efficiency, and the optimized medium and conditions improve its proliferation and metabolic stability, providing a basis for cultivation and application in treating high-strength ammonia nitrogen wastewater.

Keywords: ammonia-oxidizing bacteria; *Nitrosomonas europaea*; medium optimization; landfill leachate

1. Introduction

Ammonia-oxidizing bacteria (AOB) exhibit high substrate specificity and require stringent environmental conditions for growth. In natural environments, AOB frequently compete with heterotrophic bacteria, resulting in low isolation efficiency [1]. Due to their chemoautotrophic nature, AOB rely on specific substrates and favorable environmental conditions for growth. Even under suitable cultivation conditions, AOB generally exhibit slow growth rates, with doubling times typically exceeding 10 h. Consequently, they are readily outcompeted by fast-growing heterotrophic microorganisms, making it difficult to obtain high-purity strains using conventional isolation methods [2]. The cultivation efficiency of AOB is influenced by multiple environmental factors, among which medium composition, temperature, and the initial ammonia nitrogen concentration are particularly important.

Iron is an essential trace element in the metabolism of AOB, as it directly participates in the active centers of both ammonia monooxygenase (AMO) and hydroxylamine oxidoreductase (HAO) [3]. The chemical form of iron significantly influences the growth and metabolic activity of AOB. Ferrous iron

 doi:10.20944/preprints202605.0679.v1

(Fe^{2+}) functions as a cofactor for AMO. Insufficient Fe^{2+} concentrations may result in reduced enzyme activity, whereas excessive Fe^{2+} levels can promote the generation of reactive oxygen species (ROS) through the Fenton reaction, thereby inducing oxidative stress [4]. In addition, the sensitivity of AOB to Fe^{2+} varies among species. Compared with Fe^{2+}, ferric iron (Fe^{3+}) exhibits lower bioavailability and must first be converted into Fe^{2+} through siderophore-mediated transport or cellular reduction systems before microorganisms can utilize it. Moreover, excessive Fe^{3+} concentrations may compete with Fe^{2+} for membrane transporters, thereby inhibiting the catalytic activity of key enzymes involved in ammonia oxidation [5].

Calcium carbonate ($CaCO_3$) performs multiple functions in the cultivation of AOB. It acts as a pH buffer, thereby maintaining the alkaline conditions required for ammonia oxidation, and simultaneously provides an inorganic carbon source for CO_2 fixation by chemoautotrophic microorganisms [6]. In addition, $CaCO_3$ particles can serve as attachment sites for bacterial cells [7] and may further enhance quorum sensing processes [6]. However, the low solubility of $CaCO_3$ may adversely affect the medium composition when excessive amounts are added. Elevated Ca^{2+} concentrations can promote precipitation with phosphate ions, thereby reducing phosphorus bioavailability in the culture medium [8].

In addition to the medium composition, environmental factors, particularly temperature, exert significant regulatory effects on AOB metabolism. Temperature directly influences enzymatic reaction rates and the efficiency of cellular energy metabolism. In general, low temperatures induce physiological stress responses in AOB, resulting in reduced membrane fluidity and decreased synthesis and uptake of compatible solutes and proteins [9]. Microorganisms adapt to low-temperature conditions through several protective mechanisms, including the production of cold-responsive signaling molecules such as trehalose and cold-shock proteins [10]. However, Lu et al. [11] reported that elevated trehalose levels were not detected in Nitrosomonas europaea (N. europaea) ATCC 19718 under cold stress conditions. This finding suggests that the currently proposed cold adaptation mechanisms of N. europaea require further re-evaluation. Furthermore, Antoniou et al. [12] observed that, within the experimental temperature range of 15-25 °C, the effective maximum specific growth rate (μ_{max}) of Nitrosomonas increased from 0.12 to 0.97 d^{-1} with increasing temperature [12]. These results indicate that nitrifying bacteria generally exhibit higher growth rates at higher temperatures.

N. europaea exhibits low affinity toward ammonia but demonstrates strong tolerance to elevated ammonia nitrogen concentrations. In contrast, its growth is inhibited under conditions of low ammonia nitrogen availability [13]. However, excessively high ammonia nitrogen levels can lead to the accumulation of free ammonia (FA). The FA concentration is jointly influenced by pH and ammonia nitrogen levels. Elevated FA concentrations exert substantial inhibitory effects on the growth and metabolic activity of N. europaea [14].

The combined effects of the above-indicated factors make medium optimization essential for the successful isolation and cultivation of AOB. However, conventional culture media are primarily empirical formulations and often lack a systematic evaluation of the dynamic balance among trace elements. As a result, low isolation efficiency and limited adaptability of AOB are frequently observed. Ammonia oxidation is the rate-limiting step in the nitrification process, and its efficiency directly influences the nitrogen cycle and the operational stability of wastewater treatment systems. Environmental parameters, including temperature and initial ammonia nitrogen concentration, influence the proliferation rate and functional gene expression of AOB by regulating membrane permeability, enzyme reaction kinetics, and microbial community competition [15,16]. Therefore, based on the systematic optimization of culture medium composition, the present study investigates the effects of $CaCO_3$, Fe^{2+}, and Fe^{3+} on the growth and ammonia oxidation performance of the AOB strain N. europaea W4. Furthermore, the roles of temperature and initial ammonia nitrogen concentration in nitrogen removal performance are examined. Finally, the practical application potential of the strain is evaluated through bench-scale treatment experiments using landfill leachate. By integrating physiological and biochemical experiments with molecular biological approaches,

 doi:10.20944/preprints202605.0679.v1

including 16S rDNA analysis, this study aims to elucidate the mechanisms by which key nutritional and environmental factors influence the growth and activity of AOB. The findings are expected to provide a theoretical basis for the efficient isolation, cultivation, and industrial application of AOB.

2. Materials and Methods

2.1. Sample Source

Water samples were collected from a section of the river affected by domestic sewage discharge in Zhongshan. The samples were initially pre-filtered through a 0.45 μm nylon membrane to remove large suspended particles. Subsequently, the filtrates were centrifuged at 3000× g for 5 min, and the resulting pellets were collected for further analysis.

2.2. Media and Reagents

AOB liquid medium (pH 7) was modified based on DSMZ Medium 1583 [17]. The medium contained 0.5 g/L $MgSO_4·7H_2O$, 0.2 g/L NaCl, 0.1 g/L KH_2PO_4, 5.0 g/L $CaCO_3$, 1.5 g/L $NaHCO_3$, 0.37 g/L NH_4Cl, 0.05 g/L $FeCl_3·6H_2O$, and 0.1% trace element solution. The trace element solution consisted of 0.062 g/L H_3BO_3, 0.017 g/L $CuCl_2·2H_2O$, 0.1 g/L $MnCl_2·4H_2O$, 0.036 g/L $Na_2MoO_4·2H_2O$, 0.07 g/L $ZnCl_2$, 0.19 g/L $CoCl_2·6H_2O$, and 0.024 g/L $NiCl_2·6H_2O$. The pH of the medium was adjusted to 7.0 with 1 mol/L NaOH and 1 mol/L HCl.

2.3. Isolation and Purification of AOB

2.3.1. Strain Enrichment

The collected cell pellet was inoculated into a 250 mL conical flask containing 95 mL of AOB liquid medium. The cultures were incubated at 30 °C and 150 r/min in the dark. Ammonia nitrogen and nitrite nitrogen concentrations were measured at 12 h intervals throughout the cultivation period. Once the culture reached the logarithmic growth phase, 5 mL of the enriched culture was transferred into fresh medium for subculturing. This enrichment procedure was repeatedly performed until stable ammonia degradation and nitrite accumulation were achieved.

2.3.2. Strain Isolation

Primary screening: The AOB medium was sterilized by filtration through a 0.22 μm membrane and subsequently dispensed for later use. A 5 mL aliquot of the enrichment culture, with an initial ammonia nitrogen concentration of 100 mg/L, was inoculated into 95 mL of sterile AOB medium. The culture was incubated at 30 °C and 150 r/min in the dark until the logarithmic growth phase was reached (OD600 ≈ 0.1). Subsequently, 0.5 mL of the culture was transferred into 4.5 mL of sterile medium and thoroughly mixed. Serial 10-fold dilutions were then prepared up to 10^{-9}. Before each dilution step, the suspension was sonicated at 3000 Hz for 1 min to disperse cell aggregates. Aliquots (200 μL) from the 10^{-6} to 10^{-9} dilutions were spread onto silica gel solid plates, and blank control plates were prepared simultaneously. All plates were sealed and incubated at 30 °C in the dark for 14 days. Single colonies were subsequently selected and inoculated into 5 mL of liquid medium, then incubated statically at 30 °C for 7 days. Nitrite production was quantified using the Griess assay. Cultures exhibiting nitrite concentrations greater than 20 mg/L were selected for further purification.

Secondary screening: The positive culture obtained from the primary screening was serially diluted 10-fold. Subsequently, 500 μL aliquots from the 10^{-7} and 10^{-8} dilutions were inoculated into two separate 96-well plates. The plates were sealed with Parafilm and incubated at 30 °C in the dark for 30 days. Nitrite concentrations in the wells were determined using the Griess assay. Cultures from nitrite-positive wells were subsequently transferred into beef extract peptone medium and incubated at 30 °C in the dark for 7 days. The absence of contamination was verified based on medium clarity and microscopic observation. The isolate was then preliminarily identified as a purified AOB strain.

 doi:10.20944/preprints202605.0679.v1

2.4. Identification of AOB

2.4.1. Scanning Electron Microscopy

Cells harvested during the logarithmic growth phase were centrifuged at 3000× g for 10 min, and approximately 1 g of cell pellet was collected. The pellet was fixed with 2.5% glutaraldehyde for 4 h. After fixation, the supernatant was removed, and the cells were rinsed three times with 0.1 mol/L phosphate buffer, with each wash lasting 20 min. The samples were subsequently dehydrated using a graded ethanol series (30%, 50%, 70%, 80%, 90%, and 100%) with each step lasting 15 min. After ethanol removal, the samples were immersed in isoamyl acetate for 10 min under gentle agitation. The treated samples were then dried using a critical-point dryer, sputter-coated with gold, and finally observed and photographed using a field-emission scanning electron microscope (FE-SEM).

2.4.2. 16S rRNA Gene Sequence Analysis

The 16S rDNA gene was amplified using the universal primers 27F (5′-AGAGTTTGATCCTGGCTCAG-3′) and 1492R (5′-GGTTACCTTGTTACGACTT-3′). The polymerase chain reaction(PCR) mixture (25 μL total volume) consisted of 12.5 μL 2× Taq Master Mix (Vazyme, China), 1 μL each of forward and reverse primers (10 μM), 1 μL of template DNA, and 9.5 μL of double-distilled water (ddH_2O). The PCR amplification conditions were as follows: initial denaturation at 95 °C for 5 min; followed by 30 cycles of denaturation at 95 °C for 30 s, annealing at 55 °C for 30 s, and extension at 72 °C for 90 s. A final extension step was performed at 72 °C for 10 min. The purified PCR products were submitted to Sangon Biotech (Shanghai, China) for sequencing. The obtained sequences were analyzed using NCBI BLAST, and reference sequences with greater than 99% similarity were retrieved for comparative analysis. A phylogenetic tree was subsequently constructed in MEGA using the neighbor-joining method with 1000 bootstrap replicates.

2.5. Effects of Medium Components and Environmental Factors on the Nitrogen Removal Performance of the Strain

N. europaea W4 was used as the experimental strain and inoculated into 250 mL conical flasks containing 100 mL of sterile medium at an inoculum size of 1% (v/v). The flasks were sealed with sterile cotton plugs, and all experimental procedures were conducted under aseptic conditions in a clean bench. Except for the temperature-related experiments, all cultures were incubated at 30 °C and 150 r/min in a constant-temperature shaker. Three replicates were prepared for each treatment, together with a non-inoculated blank control. Ammonia nitrogen and nitrite nitrogen concentrations were measured every 12 h to evaluate the ammonia-oxidation performance. When required, the pH was adjusted to 7.0 using 1 mol/L NaOH and monitored using pH test paper.

2.5.1. Effect of $CaCO_3$ on the Nitrogen Removal Performance of *N. europaea* W4

Two treatment groups were established: one without $CaCO_3$ supplementation and the other with 5 g/L $CaCO_3$ supplementation. The initial ammonia nitrogen concentration in both groups was maintained at 100 mg/L. The effects of $CaCO_3$ on the ammonia-oxidizing performance of N. europaea W4 were evaluated by monitoring changes in ammonia nitrogen and nitrite nitrogen concentrations throughout the cultivation period.

2.5.2. Effects of Fe^{2+} and Fe^{3+} on the Nitrogen Removal Performance of *N. europaea* W4

The concentrations of both Fe^{2+} and Fe^{3+} were adjusted to 0.05 g/L. The effects of iron ions in different valence states on the ammonia-oxidizing performance of N. europaea W4 were compared.

2.5.3. Effect of Temperature on the Nitrogen Removal Performance of *N. europaea* W4

 doi:10.20944/preprints202605.0679.v1

Five temperature conditions were established at 10, 15, 20, 30, and 40 °C. Following inoculation, the conical flasks were incubated at the respective temperatures with shaking at 150 r/min. The initial ammonia nitrogen concentration in all treatment groups was maintained at 100 mg/L.

2.5.4. Effect of Initial Ammonia Nitrogen Concentration on the Nitrogen Removal Performance of *N. europaea* W4

The initial ammonia nitrogen concentrations were adjusted to 100, 500, 1000, 1750, and 2500 mg/L. Changes in ammonia nitrogen and nitrite nitrogen concentrations were monitored throughout the cultivation period to evaluate the effects of different ammonia nitrogen concentrations on the ammonia-oxidizing performance of N. europaea W4.

2.6. Bench-Scale Test of N. europaea W4 in Aerobic Tank Wastewater

Wastewater from the aerobic tank at a municipal solid waste transfer station in Yichang, with a treatment capacity of 100 t/d, was selected as the target for treatment. The sampling point was located at the center of the aerobic tank, approximately 1.5 m below the water surface. A composite wastewater sample (25 L) was collected in September 2023 using a sterile sampler. The collected samples were filtered through 0.45 μm membrane filters before analysis. The main water quality parameters of the wastewater are presented in Table 1.

Table 1. Water quality parameters of the landfill leachate.

Parameter	**Concentration (mg/L)**
Total nitrogen (TN)	388
Ammonia nitrogen (NH_4^+-N)	115
Total phosphorus (TP)	112
Chemical oxygen demand (COD)	5.79 × 103
Calcium ion (Ca^{2+})	31.2
Magnesium ion (Mg^{2+})	67

A 100 mL aliquot of the N. europaea W4 culture at the logarithmic growth phase was centrifuged at 3000× g to harvest the cells. The resulting cell pellet was resuspended to prepare a bacterial suspension, which was subsequently inoculated into a 250 mL conical flask containing 100 mL of landfill leachate. The cultures were incubated at 30 °C and 50 r/min in the dark. A non-inoculated control group was established simultaneously, and all treatments were conducted in triplicate. Ammonia nitrogen and nitrite nitrogen concentrations were measured every 12 h throughout the experiment.

2.7. Statistical Analysis

The nitrite accumulation rate (V, mg/(L·h)) was calculated using Eq. (1):

$$V=\frac{C_{t2}-C_{t1}}{t_2-t_1} \quad (1)$$

Where Ct1 and Ct2 represent the nitrite concentrations (mg/L) at time t1 and t2, respectively. The specific growth rate (μ, d^{-1}) was calculated using Eq. (2):

$$\mu=\frac{\ln(V_2)-\ln(V_1)}{t_2-t_1} \quad (2)$$

Where V2 and V1 represent the nitrite accumulation rates (mg/(L·h)) measured at days t2 and t1, respectively. The generation time (g, h) was calculated using Eq. (3):

 doi:10.20944/preprints202605.0679.v1

$$g=\frac{\ln 2}{\mu}\times 24 \quad (3)$$

Where μ represents the specific growth rate (d^{-1}).

Figures and graphs were prepared using Origin, and the error bars represent the standard deviation (SD). Statistical analysis was performed using SPSS. Analysis of variance (ANOVA) was conducted to evaluate statistical significance among different treatment groups.

3. Results

3.1. Isolation and Purification Results

Water samples were collected from the Shiqi River. Following enrichment cultivation at 100 mg/L initial ammonia nitrogen, pH 7, and 30 °C in the dark, a pure bacterial strain was successfully isolated using serial dilution combined with silica gel plate spreading techniques. When cultivated in a medium containing an initial ammonia nitrogen concentration of 100 mg/L for 72 h, the isolated strain achieved an ammonia nitrogen removal efficiency of 99.0%, accompanied by a nitrite accumulation of 99.2 mg/L, and an ammonia-to-nitrite conversion efficiency exceeding 99%. The culture was subsequently transferred into beef extract peptone medium and incubated at 30 °C for 7 days. No colony growth was observed during incubation, confirming that the isolate was a pure culture with no detectable contamination. The strain was deposited at the China Center for Type Culture Collection under the deposit number CCTCCM 2024693.

3.2. Identification Results

3.2.1. Scanning Electron Microscopy Results

Field-emission scanning electron microscopy (FE-SEM) observation (Figure 1) revealed that cells of N. europaea W4 in the logarithmic growth phase exhibited short rod-shaped to nearly coccoid morphologies. The dimensions of individual cells ranged from approximately 1.0–1.5 μm in length and 0.2–0.4 μm in width, which are consistent with the reported morphological characteristics of the type strain N. europaea ATCC 19718. The cell surface displayed irregular wrinkling structures, whereas flagella, pili, and capsules were not observed. In addition, the cells showed a strong tendency to aggregate rather than disperse uniformly within the culture system.

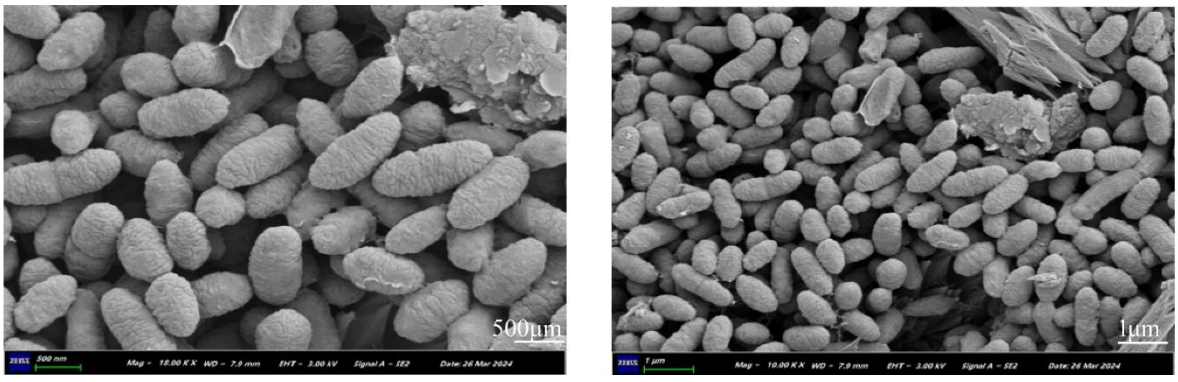

Figure 1. Morphological Characteristics of the Strain under Scanning Electron Microscope.

3.2.2. 16S rDNA Sequencing Results

The 16S rDNA gene sequence (1486 bp) of strain W4 was obtained through PCR amplification and subsequently compared with sequences in the NCBI RefSeq database using the BLASTn program. The analysis revealed that strain W4 shared the highest sequence similarity (99.93%) with N. europaea ATCC 25978 (EMBL-EBI accession number: PRJNA245576). A phylogenetic tree

 doi:10.20944/preprints202605.0679.v1

constructed based on 16S rDNA sequences further demonstrated that strain W4 clustered within the same clade as N. europaea, while forming a clearly distinct lineage from Nitrosospira (Figure 2). Therefore, the isolate was identified as N. europaea and designated as N. europaea W4.

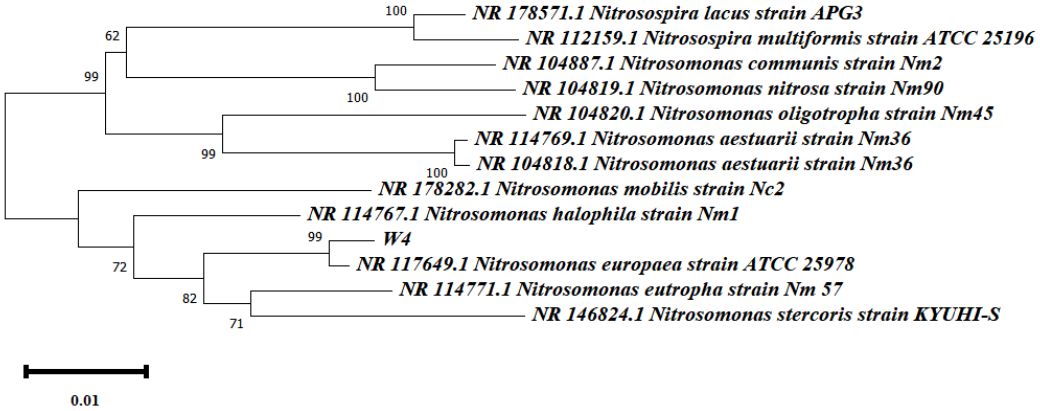

Figure 2. Strain N. europaea W4 and the phylogenetic tree constructed based on 16S rRNA gene sequence.

3.3. Effects of Medium Components, Temperature, and Initial Ammonia Nitrogen Concentration on the Nitrogen Removal Performance of the Strain

3.3.1. Effect of $CaCO_3$ on the Nitrogen Removal Performance of *N. europaea* W4

As shown in Figure 3, no evident lag phase was observed in the $CaCO_3$-supplemented group. The initial ammonia nitrogen concentration of 100.76 ± 0.63 mg/L decreased to 25.56 ± 0.49 mg/L on day 3, whereas the nitrite nitrogen concentration increased from 1.24 ± 0.02 mg/L to 72.26 ± 2.01 mg/L over the same period. The maximum specific growth rate (μ_{max}) reached 1.42 d^{-1} during days 2–3, and the logarithmic growth phase was observed from day 1 to day 3. By day 4, ammonia nitrogen concentration had declined to 1.30 ± 0.98 mg/L, indicating that ammonia oxidation was nearly complete. The final nitrite nitrogen concentration reached 98.59 ± 0.46 mg/L on day 10. In the group without $CaCO_3$ supplementation, no significant change in ammonia nitrogen concentration was observed during the first 7 days. After the culture entered the logarithmic growth phase on day 8, ammonia nitrogen concentration rapidly decreased from 86.39 ± 1.15 mg/L to 2.30 ± 1.06 mg/L by day 10. Simultaneously, the nitrite nitrogen concentration increased from 13.90 ± 2.11 mg/L to 99.60 ± 0.69 mg/L. The maximum specific growth rate (μ_{max}) reached 1.37 d^{-1} during days 9–10. Although no significant difference in the final nitrite nitrogen concentration was observed between the two treatment groups, the addition of $CaCO_3$ shortened the lag phase by approximately 7 days, indicating that $CaCO_3$ supplementation markedly accelerated the initiation of ammonia oxidation by N. europaea W4.

 doi:10.20944/preprints202605.0679.v1

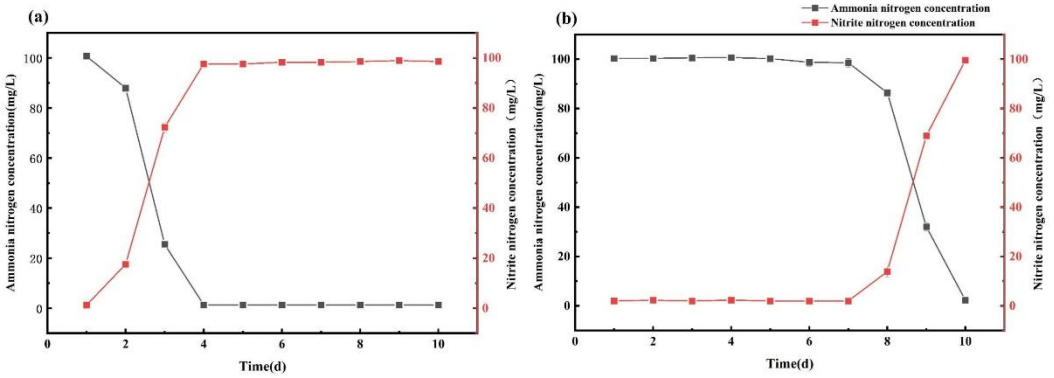

Figure 3. Effects of calcium carbonate on the growth of strain N. europaea W4. (a) Add calcium carbonate;(b) Do not add calcium carbonate.

3.3.2. Effects of Fe^{2+} and Fe^{3+} on the Nitrogen Removal Performance of *N. europaea* W4

As shown in Figure 4, the strain exhibited high ammonia-oxidizing activity in both Fe^{2+} and Fe^{3+} -supplemented media, although ammonia nitrogen consumption occurred slightly faster in the Fe^{2+} treatment group. A lag phase of approximately 1 day was observed in the Fe^{3+} group. Subsequently, the ammonia nitrogen concentration decreased from 109.28 ± 0.41 mg/L on day 1 to 2.15 ± 0.01 mg/L on day 5. In parallel, the nitrite nitrogen concentration increased from 5.26 ± 0.03 mg/L to 105.39 ± 0.01 mg/L. The maximum specific growth rate (μ_{max}) in the Fe^{3+} group reached 0.865 d^{-1} during days 2–3, and complete ammonia oxidation required approximately 5 days. In contrast, no apparent lag phase was observed in the Fe^{2+} treatment group. The ammonia nitrogen concentration decreased from 109.94 ± 0.64 mg/L to 90.30 ± 0.44 mg/L on day 1 and further declined to 4.12 ± 0.74 mg/L by day 4. Meanwhile, the nitrite nitrogen concentration increased from 3.25 ± 0.01 mg/L to 20.89 ± 0.94 mg/L on day 1 and remained stable at 108.50 ± 0.12 mg/L during days 4–6. The maximum specific growth rate (μ_{max}) reached 0.773 d^{-1} during days 1–2, and complete ammonia oxidation was achieved within only 4 days.

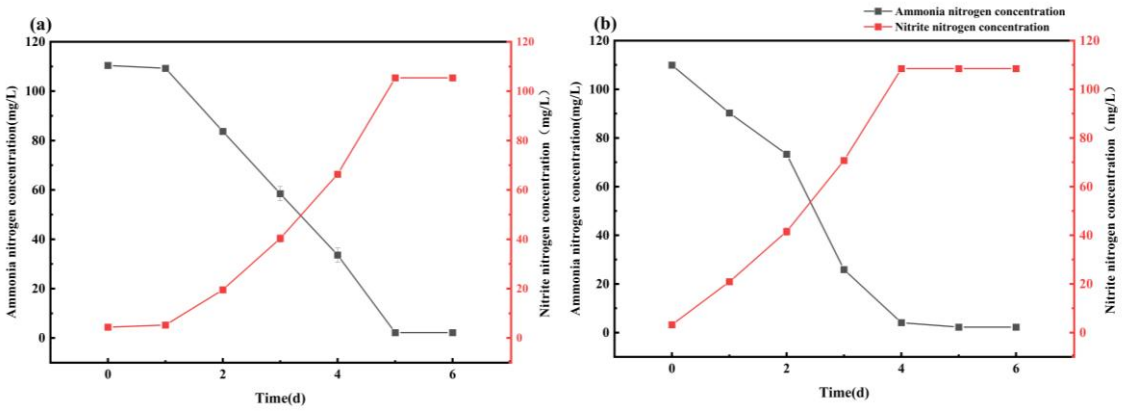

Figure 4. Effects of Fe^{2+} and Fe^{3+} on the growth of N. europaea W4（a）Fe^{3+},（b）Fe^{2+}.

3.3.3. Effect of Temperature on the Nitrogen Removal Performance of *N. europaea* W4

As shown in Figure 5, within the tested temperature range of 10–40 °C, the strain exhibited the highest ammonia-oxidizing activity at 30 °C. No apparent lag phase was observed under this condition. The ammonia nitrogen concentration decreased from 124.98 ± 0.03 mg/L to 98.9 ± 0.12 mg/L within 24 h. In contrast, negligible growth and ammonia oxidation activity were detected at the other tested temperatures. Regarding nitrite accumulation, the final nitrite nitrogen concentrations at 72 h

 doi:10.20944/preprints202605.0679.v1

reached 119.26 ± 0.01 mg/L at 20 °C and 123.45 ± 0.01 mg/L at 30 °C, with ammonia nitrogen conversion efficiencies exceeding 99% under both conditions. In contrast, only 6.02 ± 0.11 mg/L of nitrite nitrogen accumulated at 10 °C, indicating that the strain exhibited minimal proliferation and ammonia oxidation activity at low temperature. At 30 °C, more than 99% of the ammonia nitrogen was converted into nitrite within 60 h. During this period, the ammonia nitrogen concentration decreased from 124.98 ± 0.03 mg/L to 1.23 ± 0.01 mg/L, whereas the nitrite nitrogen concentration increased from 5.47 ± 0.12 mg/L to 122.45 ± 0.18 mg/L. The maximum specific growth rate reached 0.1038 h^{-1}, corresponding to a minimum generation time of 6.7 h. Fitting with the Ratkowsky 2 model showed a good correlation ($R^2 = 0.95$, $P < 0.05$) and indicated that the optimal temperature for nitrite accumulation was approximately 27 °C. In comparison, the generation time at 15 °C increased substantially to 21.7 h.

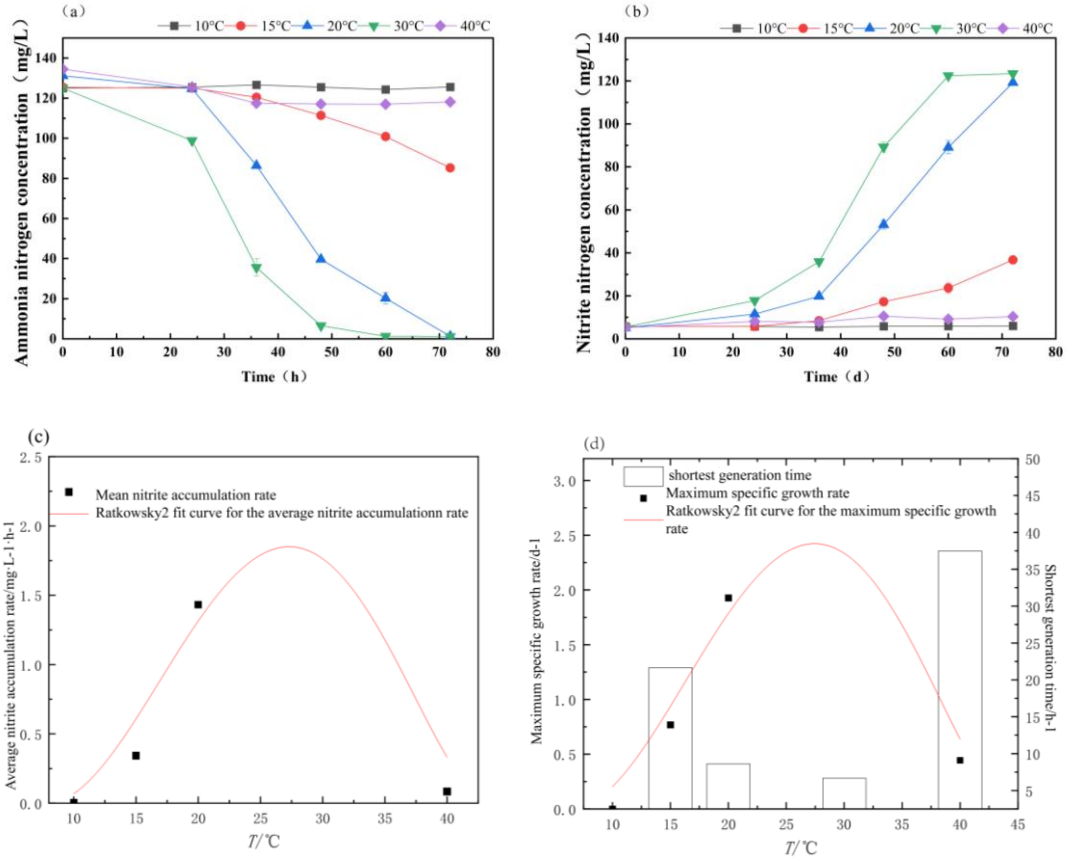

Figure 5. Effects of temperature on the denitrification performance of N. europaea W4. (a)NH4+-N,(b)NO2--N,(c)Average nitrite nitrogen accumulation rate, (d) Maximum specific growth rate.

3.3.4. Effect of Different Ammonia Nitrogen Concentrations on the Nitrogen Removal Performance of *N. europaea* W4

The effects of different initial ammonia nitrogen concentrations on the ammonia-oxidizing performance of N. europaea W4 are presented in Figure 6. In the treatment groups containing 500, 1000, and 1750 mg/L ammonia nitrogen, nitrite nitrogen accumulation was significantly higher than that observed in the other groups ($P < 0.05$). The corresponding nitrite nitrogen concentrations on day 9 reached 433.01 ± 0.32, 727.28 ± 0.89, and 760.36 ± 0.56 mg/L, respectively. These results indicate that this concentration range was the most favorable for ammonia-oxidation activity. Fitting with the Edwards 2 model demonstrated a strong correlation ($R^2 = 0.94$, $P < 0.05$) and suggested that the optimal initial ammonia nitrogen concentration for nitrite accumulation was approximately 2000 mg/L. Furthermore, the strain maintained high ammonia-oxidizing efficiency within the ammonia nitrogen concentration range of 1500–2000 mg/L.

 doi:10.20944/preprints202605.0679.v1

As the initial ammonia nitrogen concentration increased, the strain's maximum specific growth rate increased. The maximum specific growth rate observed in the 100 mg/L treatment group (0.92 ± 0.17 d^{-1}) was significantly lower than that measured in the other treatment groups ($P < 0.05$). In contrast, the maximum specific growth rates in the 1750 and 2500 mg/L groups were significantly higher than those in the low-concentration treatments ($P < 0.05$). The Edwards 2 model fitting further revealed that the effects of ammonia nitrogen concentration on ammonia oxidation activity and cellular growth in N. europaea W4 were not fully synchronized.

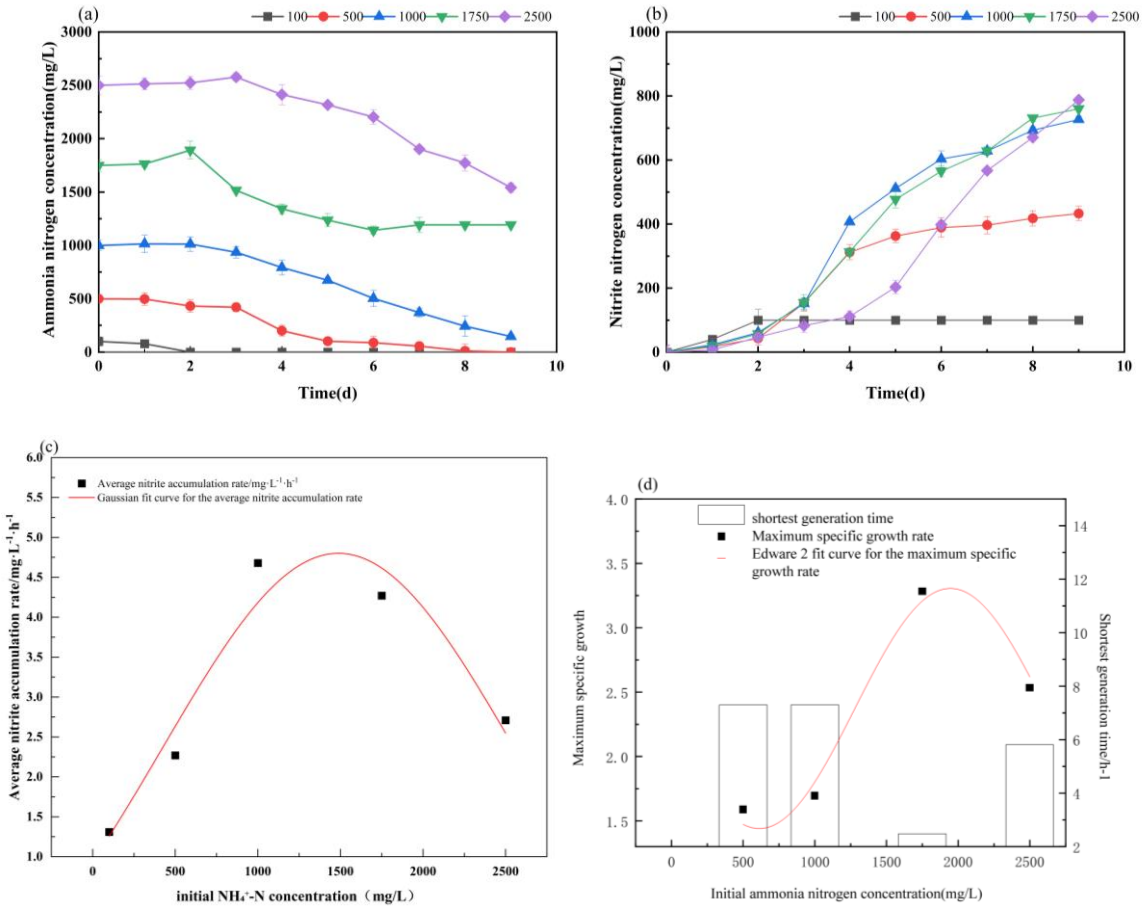

Figure 6. Effects of different ammonia - nitrogen concentrations on the denitrification performance of N. europaea W4. (a)NH4+-N,(b)NO2--N,(c)Average nitrite nitrogen accumulation rate, (d) Maximum specific growth rate.

3.4. Bench-Scale Test of N. europaea W4 in Aerobic Tank Wastewater

As shown in Figure 7, inoculation of N. europaea W4 into landfill leachate significantly enhanced ammonia nitrogen degradation. The average ammonia oxidation rate in the inoculated group reached 29.32 ± 0.07 $mg \cdot L^{-1} \cdot d^{-1}$, whereas the control group exhibited a substantially lower rate of only 4.64 ± 0.11 $mg \cdot L^{-1} \cdot d^{-1}$. No nitrite accumulation was detected in the control group throughout the experimental period. In contrast, the inoculated group showed continuous nitrite accumulation over the first 4 days, with nitrite nitrogen concentrations increasing from 29.54 ± 0.03 mg/L to a peak of 45.40 ± 0.07 mg/L on day 4. Subsequently, the nitrite concentration rapidly declined following the depletion of ammonia nitrogen.

 doi:10.20944/preprints202605.0679.v1

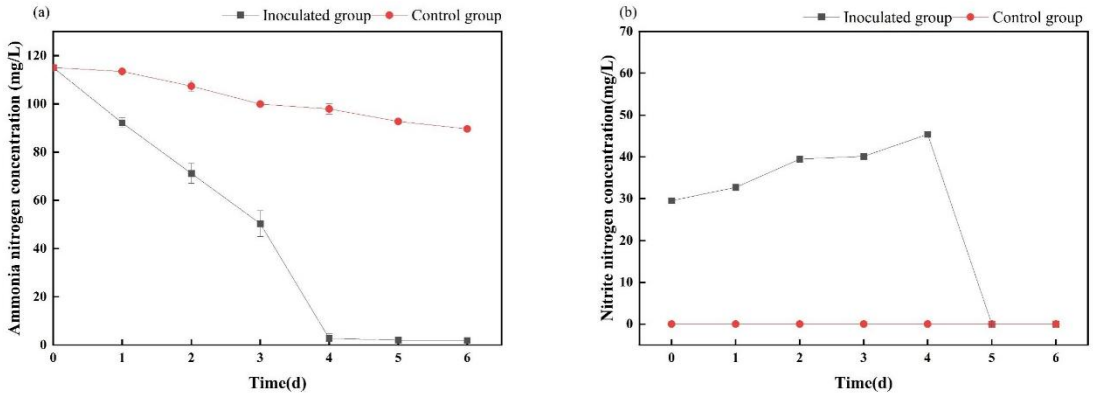

Figure 7. Bench-scale test of N. europaea W4 in aerobic tank wastewater(a)NH4+-N;(b)NO2--N.

4. Discussion

The isolation of the *N. europaea* W4 strain enriches the existing resource pool of ammonia-oxidizing bacteria (AOB) and provides valuable experimental material for investigating AOB diversity in freshwater environments in South China. Compared with the previously reported *N. europaea* ATCC 19718 [18], *N. europaea* W4 exhibits short rod-shaped to subspherical cellular morphology and shows highly phylogenetic similarity, with a 16S rDNA sequence similarity of 99.93%. However, strain W4 demonstrates distinct advantages in ammonia oxidation performance and may possess unique metabolic regulatory characteristics and environmental adaptability [19]. Phylogenetic analysis demonstrated that *N. europaea* W4 clustered within the same clade as *N. europaea* and was clearly separated from *Nitrosospira* strains. This finding not only confirms the taxonomic classification of strain W4 but also reflects the functional divergence that has occurred between *Nitrosomonas* and *Nitrosospira* during evolutionary adaptation processes. *Nitrosomonas* species are generally adapted to environments with high ammonia nitrogen concentrations, whereas *Nitrosospira* species preferentially inhabit environments with relatively low ammonia nitrogen levels [20]. *N. europaea* W4 demonstrated high ammonia oxidation efficiency in a medium containing an initial ammonia nitrogen concentration of 100 mg/L. Within 72 h, the strain achieved an ammonia nitrogen removal efficiency of 99% and a nitrite nitrogen conversion efficiency exceeding 99%.

Scanning electron microscopy (SEM) observations revealed that *N. europaea* W4 exhibited a short-rod-shaped to subspherical morphology with irregularly wrinkled cell surfaces. No cellular appendages, such as flagella, fimbriae, or capsules, were observed. These morphological characteristics may be related to the strain's planktonic growth state in the liquid medium. In addition, the strain's cell wall structure may confer specific mechanical strength and enhanced environmental adaptability. The cells tended to aggregate into clusters rather than disperse uniformly throughout the medium, suggesting that *N. europaea* W4 may regulate surface adhesion via quorum-sensing mechanisms. Such aggregation may facilitate the formation of biofilm precursors, thereby enhancing environmental tolerance and metabolic efficiency [21]. This observation provides additional experimental evidence for further investigation into the mechanisms of AOB biofilm formation.

$CaCO_3$ supplementation significantly reduced the lag phase of *N. europaea* W4 from approximately 6 days to a negligible duration, while exerting no substantial effect on the maximum specific growth rate (μ_{max}). The μ_{max} values were 1.42 d^{-1} and 1.37 d^{-1} in the $CaCO_3$ -supplemented and non-supplemented groups, respectively. Conventionally, $CaCO_3$ functions as both an acidity-neutralizing agent and an inorganic carbon source supplier. However, these functions alone cannot fully explain the observed uncoupling between lag-phase duration and the maximum specific growth rate. Wang et al. [22] reported that the combined application of calcium carbonate with specific biochar and organic fertilizers effectively stimulated soil nitrification activity, suggesting that $CaCO_3$ may exert biological functions beyond simple acid–base neutralization. Furthermore, Kolodkin-Gal

 doi:10.20944/preprints202605.0679.v1

et al. [23] noted that Ca^{2+} not only serves as a structural component involved in biomineralization but also acts as a signaling molecule that regulates gene expression and biofilm formation. Based on the above evidence, it is proposed that the mechanism by which $CaCO_3$ shortens the lag phase involves the combined effects of physical enrichment and calcium-mediated signaling. Specifically, $CaCO_3$ particles may promote local microbial enrichment through surface attachment, while released Ca^{2+} ions may independently stimulate early-stage colonization and coordinated expression of functional genes. Consequently, the time required to establish a stable microbial community is substantially reduced. The absence of a significant change in μ_{max} further supports the hypothesis that Ca^{2+} primarily regulates microbial community behavior rather than directly enhancing the metabolic rate of individual cells. The potential interaction between Ca^{2+}-mediated signaling and the quorum sensing system of AOB, as well as the specific role of $CaCO_3$ in complex microbial systems, still requires further molecular-level verification. These findings suggest that $CaCO_3$ primarily functions as a priming factor rather than a direct growth-enhancing agent in the regulation of nitrifying microorganisms. This study therefore provides valuable experimental evidence for understanding AOB growth kinetics and for optimizing nitrification processes in wastewater treatment systems.

The experimental results demonstrated that the lag phase in the Fe^{2+} treatment group was approximately 1 day shorter than that in the Fe^{3+} treatment group. In addition, the ammonia nitrogen consumption rate in the Fe^{2+}-supplemented medium was slightly higher than that observed in the Fe^{3+} medium. Fe^{2+} can be directly absorbed by AOB and incorporated into the active centers of ammonia monooxygenase (AMO) and hydroxylamine oxidoreductase (HAO). In contrast, Fe^{3+} must first undergo chelation, transport, and reduction to Fe^{2+} via siderophore-mediated pathways before it can be utilized. This reduction process imposes an additional energy burden on the cells [24]. The genome of *N. europaea* encodes a wide range of proteins associated with iron acquisition and transport [4]. The activities of AMO and HAO depend on copper/iron cofactors and heme iron cofactors, respectively. Therefore, iron availability directly affects ammonia oxidation efficiency. Under iron-limited conditions, the ammonia-dependent oxygen consumption activity of AOB decreases significantly [25]. Moreover, the transport and reduction processes required for Fe^{3+} utilization further increase the metabolic burden on the cells [26]. Consequently, under Fe^{3+} supplementation conditions, the strain is likely to allocate additional energy to Fe^{3+} reduction, leading to a lower ammonia oxidation rate and an extended lag phase [5]. Under both iron source treatments, nitrite nitrogen remained the primary end product of the AOB ammonia oxidation pathway in AOB [25]. The presence of Fe^{2+} mainly enhanced the rate of nitrite nitrogen accumulation without altering the nature of the metabolic end product.

In the present study, no release of nitrogen oxides (NO or N_2O) was detected following Fe^{2+} supplementation, and ammonia nitrogen was almost completely converted to nitrite nitrogen. Although Fe^{2+} has been reported to increase N_2O and NO emissions in non-AOB systems by promoting autotrophic denitrification, suppressing denitrification-related functional genes (e.g., nosZ), or participating in abiotic reactions with nitrite or hydroxylamine [27–29], such effects were not observed in the current experimental system. This outcome may be attributed to the use of a pure AOB culture, in which denitrifying microbial communities required for these pathways were absent. In addition, the abiotic reaction rate between Fe^{2+} and NO_2^-/NH_2OH under aerobic conditions is extremely low [30]. Therefore, within the present experimental system, Fe^{2+} primarily functioned as an essential trace element that promoted enzyme synthesis and facilitated the initiation of microbial activity, rather than inducing secondary nitrogen transformation reactions.

The optimal growth temperature range for *N. europaea* W4 was determined to be 25–30 °C. The strain still maintained basal metabolic activity at 15 °C; however, growth arrest occurred at 10 °C, indicating that further acclimation may be required to improve low-temperature tolerance. Temperature influences bacterial growth and metabolism primarily by affecting membrane fluidity, DNA replication, protein synthesis, and enzyme activity. In general, elevated temperatures enhance enzymatic activity, whereas reduced temperatures suppress metabolic processes [31]. Compared with typical AOB strains, *N. europaea* ATCC 19718 exhibits an optimal growth temperature range of

 doi:10.20944/preprints202605.0679.v1

28-32 °C [32], whereas *N. eutropha* CZ-4 has an optimal growth temperature of 30.9 °C and is capable of surviving at 40 °C [33,34]. Both strains therefore demonstrate stronger high-temperature adaptability than *N. europaea* W4. The suitable growth temperature range for AOB is generally considered to be 20-30 °C. The lower temperature tolerance limit of *N. europaea* W4 was approximately 5 °C lower than that reported for typical AOB strains, indicating that W4 possesses a relatively broad temperature adaptation range within the 15-30 °C. These temperature response characteristics suggest that *N. europaea* W4 is well suited for application in wastewater treatment systems subjected to daily temperature fluctuations between 15 and 30 °C.

N. europaea W4 exhibits low affinity toward ammonia and primarily maintains intracellular homeostasis through a high ammonia metabolic rate. When the initial ammonia nitrogen concentration increased to 2500 mg/L, the lag phase was prolonged to 72 h, approximately 48 h longer than in the moderate- and low-concentration treatment groups (100-1750 mg/L). In addition, the maximum specific growth rate decreased to 2.85 d^{-1}. This phenomenon is associated with multiple stress effects induced by high ammonia nitrogen concentrations, including disruption of intracellular ion homeostasis [35], free ammonia concentrations exceeding the inhibitory threshold for AMO activity, and increased accumulation of hydroxylamine, a by-product of ammonia oxidation that can trigger feedback inhibition [36]. Meanwhile, ammonia transporters encoded by the strain may enhance cellular tolerance to ammonia toxicity [37]. Edwards model fitting ($R^2 = 0.94$) indicated that the optimal ammonia nitrogen concentration for *N. europaea* W4 was approximately 1987 mg/L, which is substantially higher than those reported for related strains. For example, the inhibition constant (K_i) of *N. europaea* SH-3 is 922.76 mg/L, whereas those of *N. eutropha* CZ-4 and *N. halophila* C-19 are 597.88 mg/L and 186.24 mg/L, respectively [38]. Similarly, the optimal ammonia nitrogen concentration for the *N. mobilis* NZ13 enrichment culture is only 200–400 mg/L, with a half-maximal inhibitory concentration of 840 mg/L [33]. In addition, strains belonging to *N. cluster* 7 achieve their maximum growth rates at ammonium concentrations of ≥ 5 mM (approximately 70 mg/L NH_4^+) [39].

Free ammonia (FA) concentrations below 23.64 mg NH_3-N/L have been reported to promote the proliferation of AOB and stimulate extracellular polymeric substance secretion. In contrast, FA concentrations exceeding 687.1 mg/L can completely inhibit microbial activity [40,41]. *N. europaea* W4 may therefore possess unique adaptive mechanisms that enable tolerance to high nitrogen loading conditions during its evolutionary development. *N. europaea* W4 can achieve an ammonia oxidation load of 1.28-1.55 kg-N·m^{-3}·d^{-1} at ammonia nitrogen concentrations ranging from 1500 to 2000 mg/L. However, when the ammonia nitrogen concentration exceeds 2500 mg/L, it may be necessary to maintain the FA concentration below the inhibitory threshold through strategies such as stepwise dilution or pH regulation. These findings provide a theoretical foundation for the application of bioaugmentation strategies to treat industrial wastewater with high ammonia nitrogen concentrations.

N. europaea W4 exhibited measurable ammonia oxidation capacity in landfill leachate. In the inoculated treatment group, the ammonia nitrogen degradation rate was significantly enhanced, and the nitrite nitrogen concentration reached a maximum value of 45.40 mg/L. In contrast, no detectable nitrite accumulation was observed in the control group following ammonia nitrogen degradation. The high chemical oxygen demand (COD) environment (5.79×10^3 mg/L) did not completely inhibit the strain's activity. This observation may be attributable to the inherent resistance mechanisms of autotrophic AOB toward elevated organic matter concentrations [42]. Park and Noguera reported that certain AOB strains can reduce the toxicity of organic compounds by expressing efflux pump proteins [30,43]. This capability is particularly important for the biological treatment of complex wastewater matrices such as landfill leachate. The rapid decline in nitrite concentration following ammonia nitrogen depletion is likely due to synergistic interactions among multiple microbial groups. Denitrifying bacteria may utilize the high COD environment to perform dissimilatory nitrate reduction, while residual NOB may gradually recover their activity as FA concentrations decrease.

5. Conclusions

 doi:10.20944/preprints202605.0679.v1

In the present study, a highly efficient ammonia-oxidizing bacterial strain was successfully isolated from the Shiqi River. Based on morphological characterization, Gram staining, scanning electron microscopy, and 16S rDNA sequence analysis, the isolate was identified as *Nitrosomonas europaea* and designated *N. europaea* W4. Under an initial ammonia nitrogen concentration of 100 mg/L, strain W4 achieved an ammonia nitrogen removal efficiency of 99% and a nitrite nitrogen conversion efficiency exceeding 99% within 72 h. The cells of *N. europaea* W4 exhibited short rod-shaped to subspherical morphology, with wrinkled cell surfaces and no observable appendages. In addition, the cells tended to aggregate into clusters. Medium optimization experiments demonstrated that supplementation with 5 g/L $CaCO_3$ significantly reduced the strain's lag phase. The optimal growth temperature range was determined to be 25-30 °C. Although the strain maintained basal metabolic activity at 15 °C, complete growth inhibition occurred at 10 °C. Furthermore, the optimal initial ammonia nitrogen concentration was approximately 1987 mg/L, and efficient high-load ammonia treatment could be achieved within the 1500-2000 mg/L range. *N. europaea* W4 also exhibited strong tolerance to nitrite nitrogen, with no significant growth inhibition at 500 mg/L. Pilot-scale experiments using landfill leachate demonstrated that inoculation with strain W4 increased the ammonia nitrogen degradation rate by approximately 6.3-fold. In addition, the peak nitrite nitrogen concentration reached 45.40 mg/L, confirming the practical application potential of this strain in complex wastewater matrices with COD values exceeding 5.79×10^3 mg/L.

Author Contributions: Conceptualization,Y.-L.S.: Visualization, Writing—review and editing. H.-F.W.: Investigation, Writing—original draft preparation. W.-J.Z.: Data curation, Formal analysis. Z.L.: Writing—review and editing. J.G.: Project administration, Funding acquisition. F.G.: Resources.L.W.:Resources,Supervision. M.-J.L.: Conceptualization, Methodology, Writing—review and editing. All authors have read and agreed to the published version of the manuscript.

Funding: This research was funded by the National Natural Science Foundation of China (Grant No. 51579092) and the Major Science and Technology Project of China Energy Engineering Corporation Limited (Grant No. CEEC 2023-ZDYF-09).

Data Availability Statement: The datasets generated during and/or analyzed during the current study are available from the corresponding author.

Acknowledgments: The authors would like to express their gratitude to EditSprings for the expert linguistic services provided.

Conflicts of Interest: The authors declare no conflicts of interest.The authors declare no conflict of interest.

References

1. Keluskar, R.; Nerurkar, A.; Desai, A. Mutualism between autotrophic ammonia-oxidizing bacteria (AOB) and heterotrophs present in an ammonia-oxidizing colony. *Arch. Microbiol*. **2013**, *195*, 737–747. [CrossRef] [PubMed]
2. Aakra, Å.; Utåker, J.B.; Nes, I.F.; Bakken, L.R. An evaluated improvement of the extinction dilution method for isolation of ammonia-oxidizing bacteria. J. *Microbiol. Methods* **1999**, *39*, 23–31. [CrossRef] [PubMed]
3. Chain, P.; Lamerdin, J.; Larimer, F.; Regala, W.; Lao, V.; Land, M.; Hauser, L.; Hooper, A.; Klotz, M.; Norton, J.; et al. Complete genome sequence of the ammonia-oxidizing bacterium and obligate chemolithoautotroph Nitrosomonas europaea. J. *Bacteriol*. **2003**, *185*, 2759–2773. [CrossRef] [PubMed]
4. Wei, X.; Vajrala, N.; Hauser, L.; Sayavedra-Soto, L.A.; Arp, D.J. Iron nutrition and physiological responses to iron stress in Nitrosomonas europaea. *Arch. Microbiol.* **2006**, *186*, 107–118. [CrossRef] [PubMed]
5. Vajrala, N.; Sayavedra-Soto, L.A.; Bottomley, P.J.; Arp, D.J. Role of Nitrosomonas europaea NitABC iron transporter in the uptake of Fe^{3+}-siderophore complexes. *Arch. Microbiol.* **2010**, *192*, 899–908. [CrossRef] [PubMed]

 doi:10.20944/preprints202605.0679.v1

6. Yang, X.; Duan, P.; Cao, Y.; Wang, K.; Li, D. Mechanisms of mitigating nitrous oxide emission during composting by biochar and calcium carbonate addition. *Bioresour. Technol*. **2023**, *388*, 129772. [CrossRef] [PubMed]
7. Wang, T.; Flint, S.; Palmer, J. Magnesium and calcium ions: roles in bacterial cell attachment and biofilm structure maturation. *Biofouling* **2019**, *35*, 959–974. [CrossRef] [PubMed]
8. Sindelar, H.R.; Brown, M.T.; Boyer, T.H. Effects of natural organic matter on calcium and phosphorus co-precipitation. *Chemosphere.* **2015**, *138*, 218–224. [CrossRef] [PubMed]
9. Zhang, Y.M.; Rock, C.O. Membrane lipid homeostasis in bacteria. Nat. Rev. *Microbiol.* **2008**, *6*, 222–233. [CrossRef] [PubMed]
10. Kandror, O.; DeLeon, A.; Goldberg, A.L. Trehalose synthesis is induced upon exposure of Escherichia coli to cold and is essential for viability at low temperatures. Proc. *Natl. Acad. Sci.* USA **2002**, *99*, 9727–9732. [CrossRef] [PubMed]
11. Lu, H.; Ulanov, A.V.; Nobu, M.; Liu, W.T. Global metabolomic responses of Nitrosomonas europaea 19718 to cold stress and altered ammonia feeding patterns. Appl. *Microbiol. Biotechnol*. **2016**, *100*, 1843–1852. [CrossRef] [PubMed]
12. Antoniou, P.; Hamilton, J.; Koopman, B.; Jain, R.; Holloway, B.; Lyberatos, G.; Svoronos, S.A. Effect of temperature and pH on the effective maximum specific growth rate of nitrifying bacteria. *Water Res.* **1990**, *24*, 97–101. [CrossRef]
13. Bollmann, A.; Bär-Gilissen, M.J.; Laanbroek, H.J. Growth at low ammonium concentrations and starvation response as potential factors involved in niche differentiation among ammonia-oxidizing bacteria. *Appl. Environ. Microbiol.* **2002**, *68*, 4751–4757. [CrossRef] [PubMed]
14. You, Y.J. Experimental study on the inhibition effect of free ammonia (FA) on nitrifying bacteria activity. Master's Thesis, Lanzhou Jiaotong University, Lanzhou, China, **2015**. (In Chinese)
15. Koops, H.P.; Pommerening-Röser, A. Distribution and ecophysiology of the nitrifying bacteria emphasizing cultured species. FEMS *Microbiol. Ecol*. **2001**, *37*, 1–9. [CrossRef]
16. Manser, R.; Gujer, W.; Siegrist, H. Decay processes of nitrifying bacteria in biological wastewater treatment systems. *Water Res.* **2006**, *40*, 2416–2426. [CrossRef] [PubMed]
17. Koblitz, J. 1583: Medium for Ammonia Oxidizing Bacteria (Strains from Soil). Available online: https://mediadive.dsmz.de (accessed on 27 March 2026).
18. Oshiki, M.; Saito, T.; Nakaya, Y.; Satoh, H.; Okabe, S. Growth of the Nitrosomonas europaea cells in the biofilm and planktonic growth mode: responses of extracellular polymeric substances production and transcriptome. J. *Biosci. Bioeng.* **2023**, *136*, 430–437. [CrossRef] [PubMed]
19. Ye, L.; Zhang, T. Ammonia-oxidizing bacteria dominates over ammonia-oxidizing archaea in a saline nitrification reactor under low DO and high nitrogen loading. *Biotechnol. Bioeng.* **2011,** *108*, 2544–2552. [CrossRef] [PubMed]
20. Lagostina, L.; Goldhammer, T.; Røy, H.; Evans, T.W.; Lever, M.A.; Jørgensen, B.B.; Petersen, D.G.; Schramm, A.; Schreiber, L. Ammonia-oxidizing bacteria of the Nitrosospira cluster 1 dominate over ammonia-oxidizing archaea in oligotrophic surface sediments near the South Atlantic gyre. *Environ. Microbiol. Rep.* **2015**, *7*, 404–413. [CrossRef] [PubMed]
21. Decho, A.W.; Norman, R.S.; Visscher, P.T. Quorum sensing in natural environments: emerging views from microbial mats. *Trends Microbiol.* **2010**, *18*, 73–80. [CrossRef] [PubMed]
22. Wang, M.; Yang, M.; Fan, T.; Wang, D.; He, J.; Wu, H.; Si, D.; Wang, M.; Wu, S.; Zhou, D. Activating soil nitrification by co-application of peanut straw biochar and organic fertilizer in a rare earth mining soil. *Sci. Total Environ.* **2023**, *866*, 161506. [CrossRef] [PubMed]
23. Kolodkin-Gal, I.; Parsek, M.R.; Patrauchan, M.A. The roles of calcium signaling and calcium deposition in microbial multicellularity. *Trends Microbiol.* **2023**, *31*, 1225–1237. [CrossRef] [PubMed]
24. Cain, T.J.; Smith, A.T. Ferric iron reductases and their contribution to unicellular ferrous iron uptake. J. *Inorg. Biochem.* **2021**, *218*, 111407. [CrossRef] [PubMed]
25. Arp, D.J.; Stein, L.Y. Metabolism of inorganic N compounds by ammonia-oxidizing bacteria. Crit. Rev. Biochem. *Mol. Biol.* **2003**, *38*, 471–495. [CrossRef] [PubMed]

 doi:10.20944/preprints202605.0679.v1

26. Vajrala, N.; Sayavedra-Soto, L.A.; Bottomley, P.J.; Arp, D.J. Global analysis of the Nitrosomonas europaea iron starvation stimulon. *Arch. Microbiol.* **2012**, *194*, 305–313. [CrossRef] [PubMed]
27. Deng, S.; Peng, S.; Ngo, H.H.; Oanh, D.T.H.; Van Hulle, S.; Lens, P.N.L.; Guo, W. Characterization of nitrous oxide and nitrite accumulation during iron (Fe(0))- and ferrous iron (Fe(II))-driven autotrophic denitrification: mechanisms, environmental impact factors and molecular microbial characterization. *Chem. Eng. J.* **2022**, *438*, 135627. [CrossRef]
28. Zuo, J.; Fu, Q.; Hu, H.; Zhu, J. Goethite promoted N_2O emissions via increasing autotrophic nitrification dominated by ammonia oxidizing bacteria in paddy soils. *Appl. Soil Ecol.* **2024**, *201*, 105479. [CrossRef]
29. Jones, L.C.; Peters, B.; Lezama Pacheco, J.S.; Casciotti, K.L.; Fendorf, S. Stable isotopes and iron oxide mineral products as markers of chemodenitrification. *Environ. Sci. Technol.* **2015**, *49*, 3444–3452. [CrossRef] [PubMed]
30. Kampschreur, M.J.; Kleerebezem, R.; de Vet, W.W.J.M.; van Loosdrecht, M.C.M. Reduced iron induced nitric oxide and nitrous oxide emission. *Water Res.* **2011**, *45*, 5945–5952. [CrossRef] [PubMed]
31. Wang, X.; Ye, C.; Zhang, Z.; Guo, Y.; Yang, R.; Chen, S. Effects of temperature shock on N_2O emissions from denitrifying activated sludge and associated active bacteria. *Bioresour. Technol.* **2018**, *249*, 605–611. [CrossRef] [PubMed]
32. Details - Leibniz Institute DSMZ. Available online: https://www.dsmz.de/collection/catalogue/details/culture/DSM-28437 (accessed on 21 April **2026**).
33. Li, Y.; Sun, F.; Cai, Y.; Mei, H.; Cheng, K. Biological characteristics of an enrichment culture of a cold-tolerant autotrophic ammonia-oxidizing bacterium. *Environ. Sci. Technol.* (China) **2024**, *47*, 1–10. (In Chinese) [CrossRef]
34. Yang, R.; Ge, H.; Cheng, K. Cross-tolerance of Nitrosomonas eutropha CZ-4 to high-temperature and high salinity. *China Environ. Sci.* **2023**, *43*, 1378–1385. (In Chinese) [CrossRef]
35. Yang, X.; Yao, G.; Yu, J.; Zhang, H. Stress responses and protective measures of industrial microorganisms under osmotic stress. *Acta Microbiol. Sin*. **2022**, *62*, 4176–4187. (In Chinese) [CrossRef]
36. de Bruijn, P.; van de Graaf, A.A.; Jetten, M.S.M.; Robertson, L.A.; Kuenen, J.G. Growth of Nitrosomonas europaea on hydroxylamine. *FEMS Microbiol. Lett.* **1995**, *125*, 179–184. [CrossRef] [PubMed]
37. Bizior, A.; Williamson, G.; Mirandela, G.D.; Boeckstaens, M.; Marini, A.M.; Hoskisson, P.A.; Zachariae, U.; Javelle, A. Characterisation of the Rh50 protein from the ammonia-oxidising bacterium Nitrosomonas europaea. *Access Microbiol.* **2022**, *4*, acmi.ac2021.po0269. [CrossRef]
38. Cai, Y.; Xiang, S.; Cheng, K. Inhibition kinetics of ammonia nitrogen on three adsorbed Nitrosomonas strains. *Microbiol. China* **2021**, *48*, 3996–4005. (In Chinese) [CrossRef]
39. Sedlacek, C.J.; McGowan, B.; Suwa, Y.; Sayavedra-Soto, L.; Laanbroek, H.J.; Stein, L.Y.; Norton, J.M.; Klotz, M.G.; Bollmann, A. A physiological and genomic comparison of Nitrosomonas cluster 6a and 7 ammonia-oxidizing bacteria. *Microb. Ecol.* **2019**, *78*, 985–994. [CrossRef] [PubMed]
40. Jiang, Y.; Poh, L.S.; Lim, C.P.; Ng, H.Y. Effect of free ammonia inhibition on process recovery of partial nitritation in a membrane bioreactor. *Bioresour. Technol. Rep.* **2019**,*6*, 152–158. [CrossRef]
41. Sun, H.; Yu, X.; Gao, Y.; Lyu, Y.; Wang, S. Kinetic test of free ammonia (FA) inhibition on ammonia-oxidizing bacteria (AOB) activity. *Environ. Sci. (China)* **2018**, *39*, 4294–4301. (In Chinese) [CrossRef]
42. Hommes, N.G.; Sayavedra-Soto, L.A.; Arp, D.J. Chemolithoorganotrophic growth of Nitrosomonas europaea on fructose. J. *Bacteriol*. **2003**, *185*, 6809–6814. [CrossRef] [PubMed]
43. Park, S.; Ely, R.L. Candidate stress genes of Nitrosomonas europaea for monitoring inhibition of nitrification by heavy metals. *Appl. Environ. Microbiol.* **2008**, *74*, 5475–5482. [CrossRef] [PubMed]